Molecular Biology of the Cell
Vol. 20, 2254–2264, April 15, 2009

Syndapin Promotes Formation of a Postsynaptic Membrane System in *Drosophila*

Vimlesh Kumar,* Robert Fricke,† Debjani Bhar,‡ Suneel Reddy-Alla,§ K. S. Krishnan,‡§ Sven Bogdan,† and Mani Ramaswami*§‖

*Smurfit Institute of Genetics and Trinity College Institute of Neuroscience, University of Dublin Trinity College, Dublin-2, Ireland; †Institut für Neurobiologie, Universität Münster, D-48149 Münster, Germany; ‡Department of Biological Science, Tata Institute of Fundamental Research, Colaba, Mumbai 400005, India; §National Centre for Biological Sciences, Bangalore 560085, India; and ‖Department of Molecular and Cellular Biology, University of Arizona, Tucson, AZ 85721

Submitted October 28, 2008; Revised January 30, 2009; Accepted February 18, 2009
Monitoring Editor: Marcos Gonzalez-Gaitan

Syndapins belong to the F-BAR domain protein family whose predicted functions in membrane tubulation remain poorly studied in vivo. At *Drosophila* neuromuscular junctions, syndapin is associated predominantly with a tubulolamellar postsynaptic membrane system known as the subsynaptic reticulum (SSR). We show that syndapin overexpression greatly expands this postsynaptic membrane system. Syndapin can expand the SSR in the absence of dPAK and Dlg, two known regulators of SSR development. Syndapin's N-terminal F-BAR domain, required for membrane tubulation in cultured cells, is required for SSR expansion. Consistent with a model in which syndapin acts directly on postsynaptic membrane, SSR expansion requires conserved residues essential for membrane binding in vitro. However, syndapin's Src homology (SH) 3 domain, which negatively regulates membrane tubulation in cultured cells, is required for synaptic targeting and strong SSR induction. Our observations advance knowledge of syndapin protein function by 1) demonstrating the in vivo relevance of membrane remodeling mechanisms suggested by previous in vitro and structural analyses, 2) showing that SH3 domains are necessary for membrane expansion observed in vivo, and 3) confirming that F-BAR proteins control complex membrane structures.

INTRODUCTION

Membrane structure is regulated by membrane-binding proteins that interact with the underlying cytoskeleton. During endocytosis, membranes are locally deformed to create shallow invaginations that deepen into hemispherical buds, which precede the formation of tight vesicle necks where dynamin-dependent membrane scission occurs (Wigge and McMahon, 1998; Farsad and De Camilli, 2003; Zimmerberg and Kozlov, 2006). Recent findings that different F-BAR domain proteins form and stabilize membrane structures of different diameters, have contributed substantially to the molecular understanding of how this sequence of events occurs (Habermann, 2004b; Itoh *et al*., 2005; McMahon and Gallop, 2005; Tsujita *et al*., 2006; Shimada *et al*., 2007).

BAR and F-BAR/EFC proteins show in vitro liposome-tubulating activity similar to those described previously for dynamin (Stowell *et al*., 1999). However, the crescent-shaped F-BAR/EFC domains usually form wider lipid tubules, whose diameters are broadly consistent with intrinsic domain curvatures determined by x-ray crystallography (McMahon and Gallop, 2005; Shimada *et al*., 2007). Thus, F-BAR proteins FBP17 and CIP4, with an intrinsic curvature of 60 nm, form tubules whose diameter is larger than those formed by BAR domains of amphiphysin, which has a tighter intrinsic curvature of 22 nm. Therefore, F-BAR proteins may function early in the process of endocytosis to stabilize wide membrane invaginations; BAR domain proteins may help form narrower membrane necks where dynamin and membrane fission proteins function (Wigge and McMahon, 1998; Simpson *et al*., 1999; Habermann, 2004a; Peter *et al*., 2004; Itoh *et al*., 2005; Kessels and Qualmann, 2006).

Studies in cultured cells are consistent with the above-mentioned model. Overexpression of any of several F-BAR/EFC domain proteins including syndapin/Pacsin enhances formation of tubular intermediates of membrane endocytosis, particularly when their Src homology (SH) 3 domain interactions with dynamin or actin are inhibited (Itoh *et al*., 2005; Tsujita *et al*., 2006). These F-BAR protein-induced tubules in cultured cells 1) contain dynamin and known components of endocytosis; 2) are transient; and 3) are greatly elongated under conditions of dynamin or F-actin inhibition, suggesting a dynamic equilibrium between tubulation and membrane fission (Itoh *et al*., 2005; Dawson *et al*., 2006; Tsujita *et al*., 2006). Despite the elegance of existing structural, and cell biological analyses, the biological contexts in which F-BAR domain proteins function in vivo remain largely unknown. Here, we use genetic and cell biological approaches in *Drosophila* to analyze potential in vivo functions of syndapin, one of the best-known F-BAR proteins, conserved from insects to mammals (Kessels and Qualmann, 2004).

Syndapins/Pacsins, have C-terminal SH3 domains capable of binding to proline-rich domains of dynamin, and two

This article was published online ahead of print in *MBC in Press* (http://www.molbiolcell.org/cgi/doi/10.1091/mbc.E08–10–1072) on February 25, 2009.

Address correspondence to: Vimlesh Kumar (kumarv@tcd.ie) or Mani Ramaswami (mani@u.arizona.edu).

actin-regulatory proteins, WASp and synaptojanin (Kessels and Qualmann, 2002). To directly address the biological function of syndapin, we used the *Drosophila* larval neuromuscular junctions, in which one can easily study the biogenesis of a tubulolamellar postsynaptic membrane system termed the subsynaptic reticulum (SSR) (Budnik *et al*., 1996; Guan *et al*., 1996; Albin and Davis, 2004). Our results indicate that syndapin promotes formation of an endogenous tubulolamellar membrane system through a mechanism that requires both its F-BAR and SH3 domains and provides new insight into potential mechanisms and functions of F-BAR proteins in vivo.

MATERIALS AND METHODS

Fly Stocks and Culture

Flies were maintained at 25°C unless otherwise stated. All stocks and crosses were grown in standard corn meal medium (83 g/l corn flour, 50 g/l dextrose; 25 g/l sucrose; 18 g/l agar; 15 g/l yeast; 4% (vol/vol) propionic acid; 0.06% (vol/vol) orthophosphoric acid and 0.07% methyl-4-hydroxy benzene). Live yeast was later added to the vials or bottles of food. dlg^{m52} and $dpak^{11}$ were obtained from Vivian Budnik (University of Massachusetts, Amherst, MA), and Larry Zipursky (University of California Los Angeles, Los Angeles, CA), respectively. We confirmed the previous observation that $dpak^{11}$ is a protein null at the neuromuscular junction (NMJ) (Supplemental Figure S1) (Parnas *et al*., 2001). Dlg protein in dlg^{m52} mutants was severely reduced but is not a null allele (Supplemental Figure S1) (Mendoza *et al*., 2003). The isolation and characterization of *synd* mutant alleles has been described previously (Kumar *et al*., 2008).

Antibodies and Immunochemistry

Wandering third instars were pinned dorsally on a Sylgard dish and dissected in cold calcium-free HL3 saline (70 mM NaCl, 5 mM KCl, 20 mM $MgCl_2$, 10 mM $NaHCO_3$, 5 mM trehalose, 115 mM sucrose, and 5 mM HEPES, pH 7.3) to expose the neuromuscular junctions. Dissected larvae were then fixed in 3.5% paraformaldehyde in phosphate-buffered saline (PBS) containing 0.5 mM EGTA for 30 min, or in Bouin's fixative (for glutamate receptor [GluR] IIA staining) for 5 min. Larvae were then washed in PBS containing 0.15% Triton X-100, blocked for 1 h in 5% normal goat serum, and incubated overnight at 4°C with the primary antibody. Polyclonal anti-syndapin antibodies were raised in rat or rabbit against the N-terminal (SyndΔSH3, amino acids [aa] 1–377) of the protein. Affinity-purified anti-syndapin antibody was used at 1:50 dilution for immunostaining. The monoclonal antibodies anti-Dlg, anti-DGluRIIA, anti-CSP, and anti-spectrin were obtained from the Developmental Studies Hybridoma Bank (Department of Biological Sciences, University of Iowa, Iowa University, IA) and were used at 1:50 dilution. Anti-Wsp was a gift from Eyal Schejter (Weizmann Institute of Science, Rehovot, Israel) and was used at 1:200 dilution. Polyclonal anti-dPAK was a gift from Chihiro Hama (National Institute of Neuroscience, Tokyo, Japan) and was used at 1:500 dilution. Polyclonal rabbit anti-Dlg was a gift from Vivian Budnik and was used at 1:1000 dilution. Polyclonal anti-Syt was a gift from Hugo Bellen (Baylor College of Medicine, Houston, TX) and was used at 1:1000, and anti-dynamin was used at 1:200. Secondary antibodies coupled to Alexa Fluor 488 or Alexa Fluor 555 (Invitrogen, Carlsbad, CA) was used at 1:400 dilution. Stained larval preparations were mounted in VECTASHIELD (Vector Laboratories, Burlingame, CA) and imaged with a laser scanning confocal microscope (LSM510 Meta; Carl Zeiss, Jena, Germany).

Western Blotting

Fly heads were homogenized in 1× SDS sample buffer (50 mM Tris-Cl, pH 6.8, 2% SDS, 2% β-mercaptoethanol, 0.1% bromphenol blue, and 10% glycerol), boiled for 5 min, and 2 fly head equivalents of protein was fractionated on a 13.5% SDS-polyacrylamide gel electrophoresis. The protein was transferred onto polyvinylidene difluoride membrane and blocked for 1 h in 5% fat-free milk. The anti-syndapin antibodies were used at 1:10,000 dilutions. The horseradish peroxidase (HRP)-coupled secondary antibody (GE Healthcare, Chalfont St. Giles, Buckinghamshire, United Kingdom) was used at 1:50000 dilutions. Signals were detected using enhanced chemiluminescence system.

Cell Culture and Transfection

Drosophila S2R+ cells were propagated in 1× Schneider's *Drosophila* media (Invitrogen) supplemented with 10% fetal bovine serum, 50 U/ml penicillin, and 50 μg/ml streptomycin in 75-cm^2 T-flasks (Sarstedt, Rommelsdorfer Starbe, Germany) at 25°C. *Drosophila* Schneider S2R+ cells (3×10^5) were transiently cotransfected with pUAST constructs (1.1 μg) and Act5C-GAL4 DNA (0.6 μg) by using FuGENE reagent (Roche Diagnostics, Indianapolis, IN) as described previously (Bogdan and Klambt, 2003). For confocal spinning-disk imaging microscopy, cells were replated on chambered coverglass (Nalge Nunc International, Rochester, NY) pretreated with concanavalin A.

Generation of Transgenic Flies

The Synd Open Reading Frame was amplified using cDNA (EST clone, LD46328) as template. The amplicon was cloned at EcoRI and NotI site in pUAST. The enhanced yellow fluorescent protein (EYFP)-syndapin constructs were generated by polymerase chain reaction (PCR) amplification of various syndapin domains (synd full-length, 1-494 aa; synd FCH, 1-150 aa; synd F-BAR, 1-300 aa; and synd SH3, 406-494 aa) and cloned into *Drosophila* Gateway vector (developed by Murphy laboratory, Carnegie Institution of Washington, Baltimore, MD). All constructs were confirmed by sequencing for the absence of any point mutations. For generating constructs with substituted amino acids, site-directed mutagenesis was performed (Mutagenex, Piscataway, NJ) on the wild-type syndapin construct and cloned into pUAST vector. The embryonic transformation of *Drosophila* was performed by Genetic Services (Cambridge, MA). Several transgenes harboring the construct were obtained and all of them expressed Synd protein at high levels.

Electron Microscopy

Third instar larval body muscles were dissected in cold Ca^{2+}-free HL3 medium. The samples were fixed in Ca^{2+}-free Trump's fixative (pH 7.2, 4% paraformaldehyde, 1% glutaraldehyde, 100 mM cacodylate, 2 mM sucrose, and 0.5 mM EGTA) in the dissection chamber for ~30 min at room temperature. The segments A2 and A3 were dissected out and further fixed overnight at 4°C. The samples were rinsed in 0.1 M cacodylate buffer with 264 mM sucrose, postfixed in 2% osmium tetroxide, and stained en bloc during ethanol dehydration with 2% uranyl acetate. Muscles embedded in Araldite were sectioned at 60 nm. Sections stained with 2% uranyl acetate and 1% lead citrate were examined with a 100CX transmission electron microscope (JEOL, Tokyo, Japan.

Quantitation and Morphometric Analyses

Fluorescence imaging was carried out using a laser scanning confocal microscope (LSM510 Meta; Carl Zeiss). All the control and experimental samples were processed in the same way, and the same setting was used for acquiring the images. Type I boutons were imaged at 63×, and the average florescence intensity of syndapin around boutons was calculated using MetaMorph software (GE Healthcare). For calculation of SSR width and bouton area, NMJs labeled with anti-Synd and anti-HRP were imaged at 63× with zoom 4 on the confocal microscope, and the maximal intensity projection image was obtained. Although anti-HRP labels some extra bouton epitopes, the bouton boundary could be unambiguously identified under immunofluorescence microscope. The SSR width was calculated as a difference between widths of total synapse (bouton + SSR) across the bouton and the width of the bouton. Only type I boutons at muscle 6/7 from four or more animals were used for quantitation. For quantification of SSR complexity, electron micrographs were printed at 25,000× and the number of membrane segments crossing a line of 0.5 μm was manually counted. For each bouton, four to six measurements were taken, averaged, and expressed as membrane layers/micrometer.

RESULTS

Syndapin Is Localized to the Subsynaptic Reticulum and Promotes its Biogenesis

In mammalian neurons, syndapin is predominantly localized to the postsynaptic dendritic spines where it regulates endocytosis of *N*-methyl-D-aspartate receptor subtypes (Perez-Otano *et al*., 2006). Consistent with these observations, *Drosophila* syndapin is predominantly postsynaptic at the *Drosophila* third instar larval neuromuscular junction. At the postsynapse, it is tightly localized to the tubulolamellar SSR (Figure 1, A–C). Synd strongly colocalizes with the actin-regulatory protein Wsp (Figure 1, D–F) and is encircled by spectrin immunoreactivity (Figure 1, G–I), consistent with the prior observation that spectrin surrounds the SSR (Pielage *et al*., 2006). Unlike Amphiphysin, syndapin is not visible in muscle T-tubules (Razzaq *et al*., 2001; Lee *et al*., 2002) (Supplemental Figure S1).

A strong enrichment of Synd in the SSR suggested a function in generating or organizing this highly tubulolamellar postsynaptic membrane network. Thus, we asked whether loss or gain of Synd has any effect on SSR biogenesis or morphology. Although loss-of-syndapin has no effect

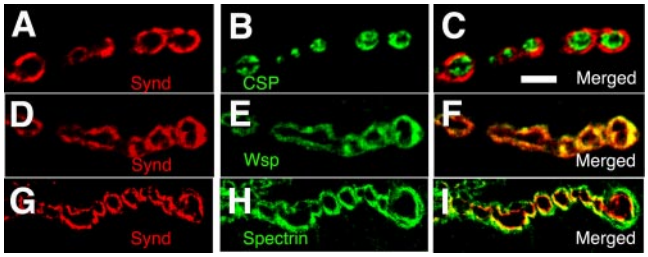

Figure 1. Syndapin localizes postsynaptically with Wsp at the *Drosophila* larval neuromuscular junction. (A–C) Single section confocal image (0.2 μm in thickness) of wild-type type I synaptic boutons of muscles 6/7 coimmunolabeled with anti-Synd (red) and anti-CSP (green) antibodies. CSP is a synaptic vesicle-associated protein and labels the presynaptic boutons at the NMJs (Zinsmaier *et al*., 1990, 1994). Note that syndapin surrounds CSP immunoreactivity. (D–F) Single confocal section of type I synaptic boutons of wild-type animal double labeled with anti-Synd (red) and anti-Wsp (green) antibodies. (F) Merged image of D and E, which reveals colocalization of syndapin and Wsp within the postsynaptic domain. (G–I) Single confocal image of wild-type NMJ double labeled with anti-Synd (red) and anti-α spectrin (green) antibodies. (I) Merged image of G and H showing that the spectrin immunoreactivity surrounds the syndapin reactivity. Bar, 5 μm (in C) for A–I.

on the gross morphology of the SSR, as judged from Dlg immunostaining of control and *synd* loss-of-function NMJ (Figure 2, A–C), a role for Synd in SSR formation, was supported by observations made in gain-of-function NMJ.

By using *Tubulin* promoter driven or *mef2* driven *Gal4*, we overexpressed a UAS-syndapin transgene either iniquitously or specifically in postsynaptic muscles. Ubiquitous or postsynaptic syndapin overexpression strongly increased syndapin immunofluorescence around SSR-rich types I but not at SSR-poor type II or type III boutons (Atwood *et al*., 1993) (Supplemental Figure S2). Quantitative analysis indicated that the width of Synd-immunoreactive regions, which correlates with SSR expansion in the vicinity of boutons is increased about twofold after muscle expression, whereas bouton size remained unchanged (Figure 2, D–K; Table 1). In addition, *UAS-synd; mef2-Gal4* larvae reared at 29°C, a temperature that allows more robust Gal4-mediated expression, not only expanded syndapin-immunopositive regions at postsynaptic sites but also spread to flanking "extrasynaptic" zones that were bereft of presynaptic innervation in "flares" of unique appearance (Figure 2, D–I).

Further analyses revealed that regions of increased syndapin immunoreactivity were, in fact, expansions of subsynaptic reticulum. First, the membrane label FM1-43 clearly marks the expanded synaptic and extrasynaptic syndapin domains (Figure 3, A–C). Similar observations were made with alternative membrane stains, AM1-43 or postsynaptically expressed, membrane-targeted green fluorescent protein (data not shown).

We confirmed the conclusion that syndapin induces SSR by using electron microscopy (EM). In the wild-type larval NMJ; boutons are surrounded by an extensive tubulolamellar infoldings of muscle membrane (Figure 3D). Syndapin overexpression resulted in an obvious expansion of postsynaptic membrane similar in morphology but different complexity to the wild-type SSR (Figure 3, E and F). To quantify the SSR complexity, we counted the number of membrane

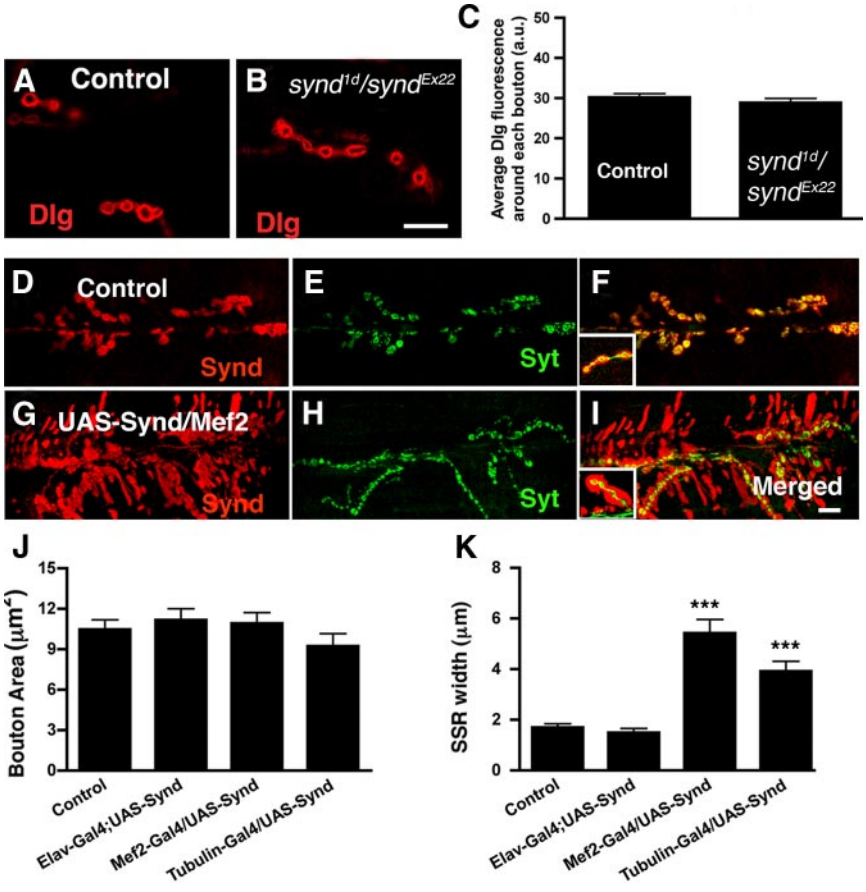

Figure 2. Overexpression of Syndapin in muscles result in expansion of syndapin-immunopositive regions at the NMJs. (A and B) Single confocal image of muscle 6/7 of wild-type (A) or synd heteroallelic ($synd^{Ex22}/synd^{1d}$) (B) mutant NMJs stained with Dlg. (C) Bar graph showing quantification of average Dlg immunofluorescence around each bouton. (D–F) Confocal projections of wild-type NMJs at muscle 6/7 costained with anti-Synd (red) and anti-HRP (green) antibodies. (F) Merged image of syndapin and HRP immunoreactivities. (G–I) Confocal projections of NMJ overexpressing syndapin, costained with anti-Synd (red) and anti-HRP (green) antibodies. Note that the overexpression of a single copy of syndapin transgene in muscle (*UAS-Syndapin; Mef2-Gal4*) results in dramatic expansion of syndapin-immunopositive reactivity around the boutons (see insets in F and I). (J) Histogram showing bouton area (area marked by anti-HRP staining) in the following genotypes: wild-type control (10.5 $\pm$ 0.72 μm^2; 21 boutons, 4 animals), *Elav-Gal4; UAS-Synd* (11.6 $\pm$ 0.95 μm^2; 19 boutons, 4 animals), *UAS-Synd/Mef2-Gal4* (11.1 $\pm$ 0.77 μm^2; 16 boutons, 4 animals), and *UAS-Synd/Tubulin-Gal4* (9.7 $\pm$ 0.89 μm^2; 13 boutons, 4 animals). (K) Histogram showing the width of synaptic SSR (width of Synd staining $-$ width of bouton) in the following genotypes: wild-type control (1.7 $\pm$ 0.15 μm; 20 boutons, 4 animals), *Elav-Gal4; UAS-Synd* (1.49 $\pm$ 0.17 μm; 19 boutons, 4 animals), *UAS-Synd/Mef2-Gal4* (5.4 $\pm$ 0.54 μm; 18 boutons, 4 animals), and *UAS-Synd/Tubulin-Gal4* (3.92 $\pm$ 0.39 μm; 13 boutons, 4 animals). Bar, 15 μm. Error bars represent SEM calculated using two-tailed *t* test.

Table 1. Quantitation of NMJ parameters in control (W^{1118}) and syndapin overexpressors based on optical imaging

	W^{1118}	Elav-Gal4; UAS-syndapin	Mef2-Gal4/ UAS-syndapin	Tubulin-Gal4/ UAS-syndapin
Avg syndapin fluorescence around boutons (a.u.)	88.7 ± 3.9 (23)	84.3 ± 3.47 (20)	177.7 ± 3.64 (34)	174.56 ± 4.1 (30)
Bouton width (μm)	3.09 ± 0.11 (19)	3.1 ± 0.14 (19)	2.86 ± 0.16 (18)	2.74 ± 0.11 (16)
SSR width (μm)	1.7 ± 0.15 (20)	1.49 ± 0.17 (19)	5.4 ± 0.54 (18)	3.92 ± 0.39 (13)
SSR width/bouton width	0.56 ± 0.05 (20)	0.51 ± 0.01 (19)	1.93 ± 0.16 (18)	1.58 ± 0.13 (16)

Values in parentheses represent the number of type Ib synaptic boutons used for quantitation. For each genotype, terminal boutons at muscle 6/7 were sampled from four different animals. The SSR width was calculated as a difference between width of total synapse (bouton + SSR) marked by syndapin and the width of the bouton marked by HRP. The errors are SEM calculated by two-tailed *t* test.

layers per micrometer in control and syndapin-overexpressing NMJ. We found that the syndapin-overexpressing animals have more complex SSR compared with wild-type controls (13.7 ± 1.6 membrane layers/micrometer for controls compared with 20.33 ± 1.8 membrane layers/micrometer for Mef2-Gal4; UAS-Syndapin, $p > 0.022$ or 19 ± 1.23 membrane layers/micrometer for Tubulin-Gal4; UAS-Syndapin, $p > 0.023$ (Figure G). Furthermore, in addition to local expansion of postsynaptic SSR, EM revealed extensions of SSR along the muscle fiber, away from sites of presynaptic innervation (Supplemental Figure S3). This is consistent with observations with lipophilic dyes, which also indicate that these extrasynaptic Synd domains contain dense membrane. Together, these data strongly suggests that overexpression of syndapin, a normal component of the SSR, is sufficient to specifically promote the biogenesis of an endogenous, postsynaptic membrane system. In addition, these findings suggest that SSR can be induced >20 μm distant from the site of presynaptic innervation. To test for any potential defect in synaptic transmission, we performed electrophysiological recording on NMJs overexpressing syndapin in muscles. We found that despite striking alterations in NMJ structure, these synapses function normally (Supplemental Figure S3).

Synaptic and Extrasynaptic Membrane Expansions Contain Native Markers of SSR

We further asked whether key components of the native SSR were present in the expanded synaptic and extrasynaptic SSR observed after syndapin overexpression. Three of these proteins are Dlg, dPAK, and WASp.

Dlg was present in both synaptic and extrasynaptic SSR, although at somewhat lower density in extrasynaptic regions (Figure 4, A–C). dPAK was also strongly recruited to the expanded SSR, being present not only in postsynaptic puncta but also in extrasynaptic regions bereft of presynaptic terminals (Figure 4, D–F). In addition, Wsp immunoreactivity was greatly increased around the boutons and strong immunoreactivity was observed in the extrasynaptic regions (Figure 4, G–I). Interestingly, postsynaptic glutamate receptor levels and distribution was not altered after SSR expansion. In the wild-type NMJ, GluR is present in a postsynaptic domain that excludes Synd (Supplemental Figure S2). Synd overexpression does not alter the GluR containing domain, but specifically expands GluR free SSR (Figure 4, J–L).

In conclusion, a variety of optical and EM analyses of NMJ show that overexpression of Synd induces a striking expansion of SSR.

Syndapin-mediated SSR Expansion Occurs in dlg and dpak Mutants

The observation that Synd expands Dlg- and dPAK-containing membranes suggested that Synd could recruit the signaling proteins dPAK and Dlg, which in turn induce SSR formation via a yet unknown pathway (Lahey *et al*., 1994; Parnas *et al*., 2001; Albin and Davis, 2004). An alternative model is that Synd, when appropriately targeted to postsynaptic sites, acts directly on the membrane to induce tubulation and SSR formation. This second model is more consistent with the in vitro activity of F-BAR proteins (Itoh *et al*., 2005; Tsujita *et al*., 2006).

Genetic epistasis experiments to discriminate between these two models of Synd action showed that Synd could induce postsynaptic membrane expansions even in dlg^{m52} and $dpak^{11}$ mutants that show highly reduced SSR (Figure 5). Thus, these data argue for a mechanism in which Synd acts parallel to or downstream of Dlg and dPAK, perhaps directly on membrane as suggested by recent studies of F-BAR family proteins. We tested a prediction of this alternative model.

F-BAR-Membrane Interactions Are Required for SSR Expansion

We first asked whether *Drosophila* syndapin induced membrane tubulation in cultured cells as predicted by its homology to previously studied F-BAR proteins. We further asked whether this conserved ex vivo activity requires the predicted protein domains and conserved amino acid residues. We then asked how these Synd variants affected SSR formation in vivo.

To test whether the cellular properties of Synd is conserved to other F-BAR domain proteins, we expressed EYFP-tagged domains of syndapin in S2-cells and analyzed their ability to form tubules. As shown in Figure 6, whereas full-length syndapin produced only weak tubulation, consistent with Itoh *et al*., 2005, the F-BAR domain (1-300 aa) induced massive tubule formation in cultured cells. In contrast, the FCH domain (1–150 aa) or the SH3 domain (406-494 aa) of syndapin had no visible effect on membrane tubulation.

Sequence alignment of Synd with other F-BAR domains showed that positively charged residues in its N-terminal F-BAR domain predicted to interact with membrane phospholipids were highly conserved (Supplemental Figure S4). Point mutations in these positively charged residues (*K63E*, *K64E*, and *R129E*, *K130E*) strongly compromised its ability to form tubules in S2 cells (Figure 6B). Thus, *Drosophila* Synd interacts with and modifies membranes ex vivo through conserved molecular mechanisms (Itoh *et al*., 2005; Tsujita *et*

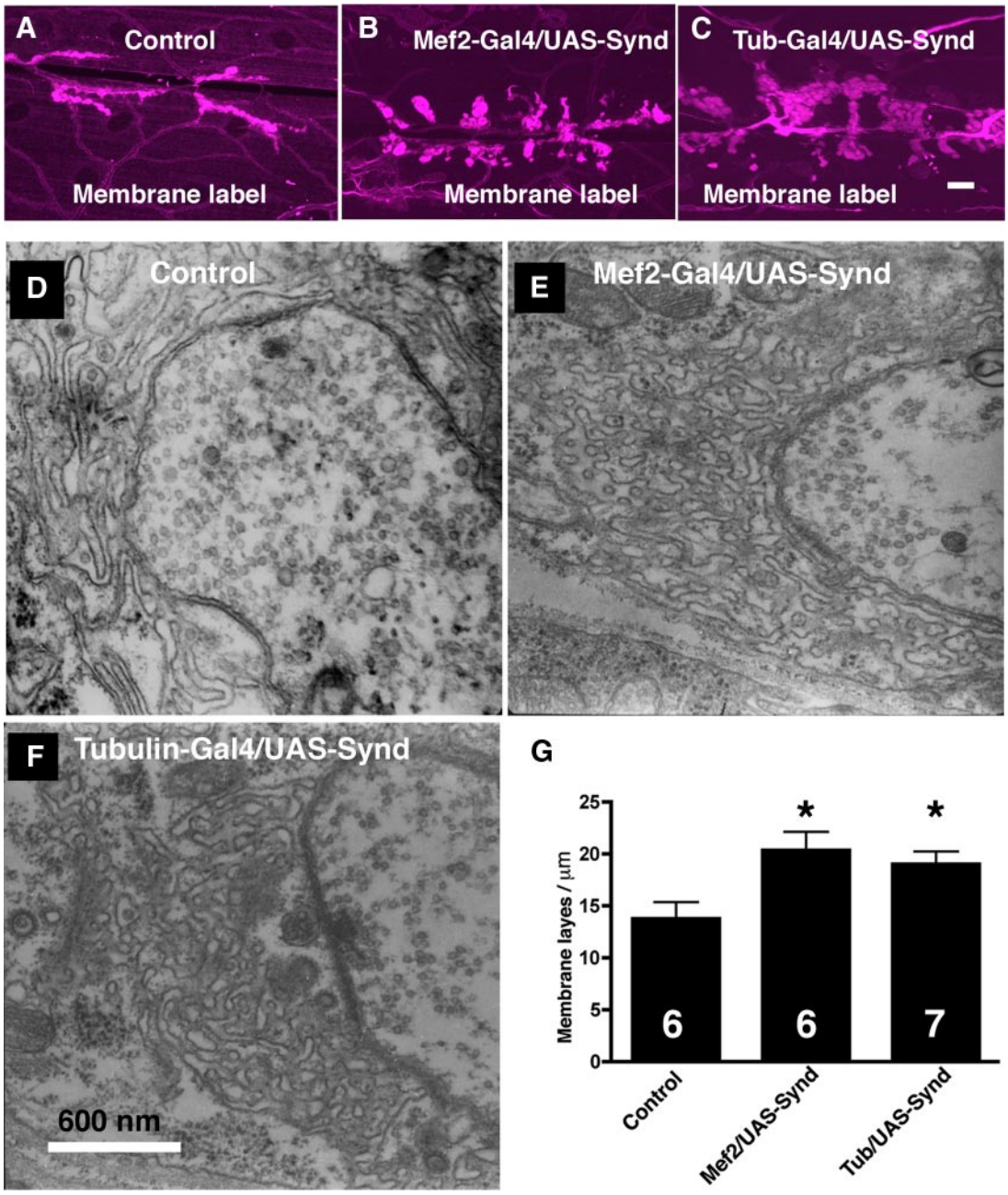

Figure 3. Syndapin overexpression induces synaptic and extrasynaptic muscle membrane folds. (A–C) Membrane-rich structures at the NMJ visualized with a lipophilic dye, FM1-43 in wild-type (A) and syndapin-overexpressing (B and C) animals. The NMJ preparations of appropriate genotypes were soaked in Ca^{2+}-free HL3 containing 1 μM FM1-43 and imaged after 1 min. Bar, 20 μm (in C) for A–C. (D–G) Electron micrographs of type 1 motor synapses in wild-type (D), *Mef2-Gal4/UAS-syndapin* animals overexpressing syndapin in muscle (E), and *Tubulin-Gal4/UAS-syndapin* animals with ubiquitous Synd overexpression (F). (G) Quantification of SSR complexity represented as number of membrane layers per micrometer for the indicated genotypes. The number in bar graphs represents number of boutons analyzed. Bar, 600 nm (in F) for D–F. Asterisk (*) represents $p > 0.02$. Error bars represent SEM calculated using two-tailed *t* test.

al., 2006). We then asked how these syndapin variants affected Synd targeting and SSR formation in vivo.

We generated transgenic flies expressing deletion constructs or selected mutant forms of Synd in postsynaptic muscle. Full-length EYFP-tagged Synd, which had weak tubulation effect in S2 cells, behaved identically to wild-type Synd in its localization and robust effect on SSR expansion (Figure 7, A–C and G–I). The Synd FCH (1–150 aa) and Synd SH3 domains (406–494 aa) were not targeted to the NMJ and had no effect on postsynaptic membrane morphology (data not shown). Interestingly, the F-BAR domain (1-300 aa), although not efficiently targeted to the postsynapse, induced patches of dense membrane randomly distributed over the muscle surface (Figure 7, D–F and J–L). These data suggest that 1) membrane modeling activity of syndapin is contained in the F-BAR domain; 2) Synd targeting to the postsynapse requires both its F-BAR and the SH3 domains; and 3) in contrast to its effect on membrane tubulation in

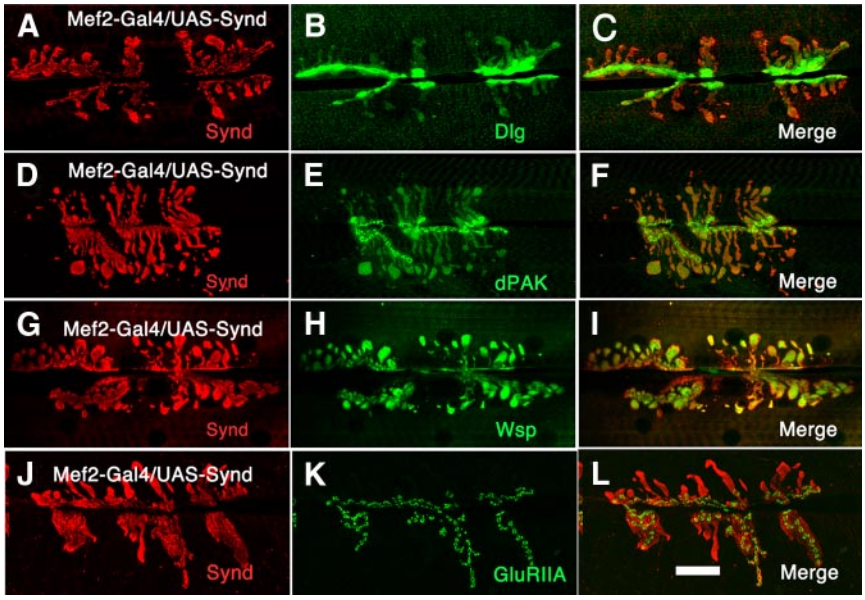

Figure 4. Recruitment of postsynaptic structural and signaling molecules at the synaptic and extrasynaptic SSR. Confocal projections of third instar NMJ overexpressing syndapin in muscles (*Mef2-Gal4/UAS-syndapin*), stained for syndapin and Dlg (A–C), dPAK (D–F), Wsp (G–I), and GluRIIA (J–L). In syndapin overexpressors, Dlg, Wsp, and dPAK but not GluRIIA follows syndapin to the membrane-rich extrasynaptic regions. Bar, 25 μm (in L) for A–L.

cultured cells, full-length Synd, when appropriately targeted, is capable of substantial membrane remodeling.

To ask whether postsynaptic membrane expansions require Synd–membrane interactions, we tested whether *syndapin*^{K63EK64E} or *syndapin*^{R129EK130E} mutants, defective in phospholipid binding, were capable of SSR expansion. Overexpression of these mutant transgenes at levels comparable with the control wild-type transgenes had no effect on synaptic or extrasynaptic SSR (Figure 8). Indeed, these mutant syndapins seemed to accumulate in the cytoplasm, consistent with a mechanism in which membrane binding is required for SSR retention (or targeting) of Synd. Thus, residues essential for the F-BAR domain to bind and tubulate membranes in vitro are necessary for syndapin's ability to expand the SSR.

DISCUSSION

Structural, cell biological, and in vitro studies of F-BAR domain proteins have contributed significantly toward our molecular understanding of how these proteins interact with membranes and other endocytic proteins to generate membrane tubules (Itoh *et al*., 2005; Tsujita *et al*., 2006; Shimada *et al*., 2007; Frost *et al*., 2008; Takano *et al*., 2008). However, our knowledge of these proteins in vivo, in the multicellular context, remains very limited. Here, we provide an in vivo analyses of syndapin in the context of its role in the biogenesis of subsynaptic reticulum, a unusual complex membrane system. We make three key observations on *Drosophila* syndapin: 1) we show that syndapin can promote formation of a tubulolamellar membrane system in vivo, 2) syndapin causes membrane remodeling that can occur without accompanying membrane fission, and 3) syndapin promotes SSR expansion by using evolutionarily conserved amino acids in its F-BAR domain. We consider these three points in turn below.

Syndapin Promotes SSR Expansion

The SSR is a unique system of tubules and lamellae formed by extensive infoldings of the postsynaptic muscle membrane; thus, in organization, they are quite different from the relatively simple F-BAR–induced membrane tubules described in cultured cells. The SSR surrounds large boutons at the *Drosophila* NMJ. Although, a role for signaling and scaffolding proteins such as dPAK and Dlg has been demonstrated in the formation of SSR, mechanisms that underlie biogenesis of this complex membrane system are still poorly understood.

Syndapin overexpression in muscle caused induction of synaptic and extrasynaptic membrane-dense subsynaptic reticulum, based on optical and electron microscopic analyses. In particular, EM sections of membrane structures induced by syndapin overexpression showed not only circular/elliptical profiles expected for tubules, but also longer parallel membrane profiles, suggesting sections through lamellae as indeed is seen for native SSR. To our knowledge, this is the first demonstration that an F-BAR protein can promote the formation of lamellar membrane infoldings. The mechanism by which syndapin may promote lamella formation is unclear, but it is likely that this arises from context specific interactions with other protein components of the SSR (Shibata *et al*., 2006; Gorczyca *et al*., 2007).

Syndapin seems to induce SSR through mechanisms that are either downstream of, or independent of, dPAK and Dlg function. This is indicated by three observations. First, the syndapin immunoreactivity is significantly reduced in dPAK and Dlg mutants (Supplemental Figure S1). Second, unlike Dlg that can induce SSR when expressed either pre- or postsynaptically, syndapin acts in a cell-autonomous manner in postsynaptic muscle. This could indicate either a function downstream of these signaling molecules or an entirely independent mechanism. The third observation is that although Synd-induced membrane is strikingly similar to the endogenous SSR in general appearance; it has some notable differences from the endogenous SSR in structure and composition. Synd-induced SSR has more densely packed membranes (~30% more membrane layers per micrometer) and also contains lower amounts of Dlg and dPAK than the endogenous SSR. Both of these differences could conceivably arise from limiting amounts of Dlg, dPAK or some other factor(s) required for the precise organization of the SSR; however, our current data do not address this issue unequivocally.

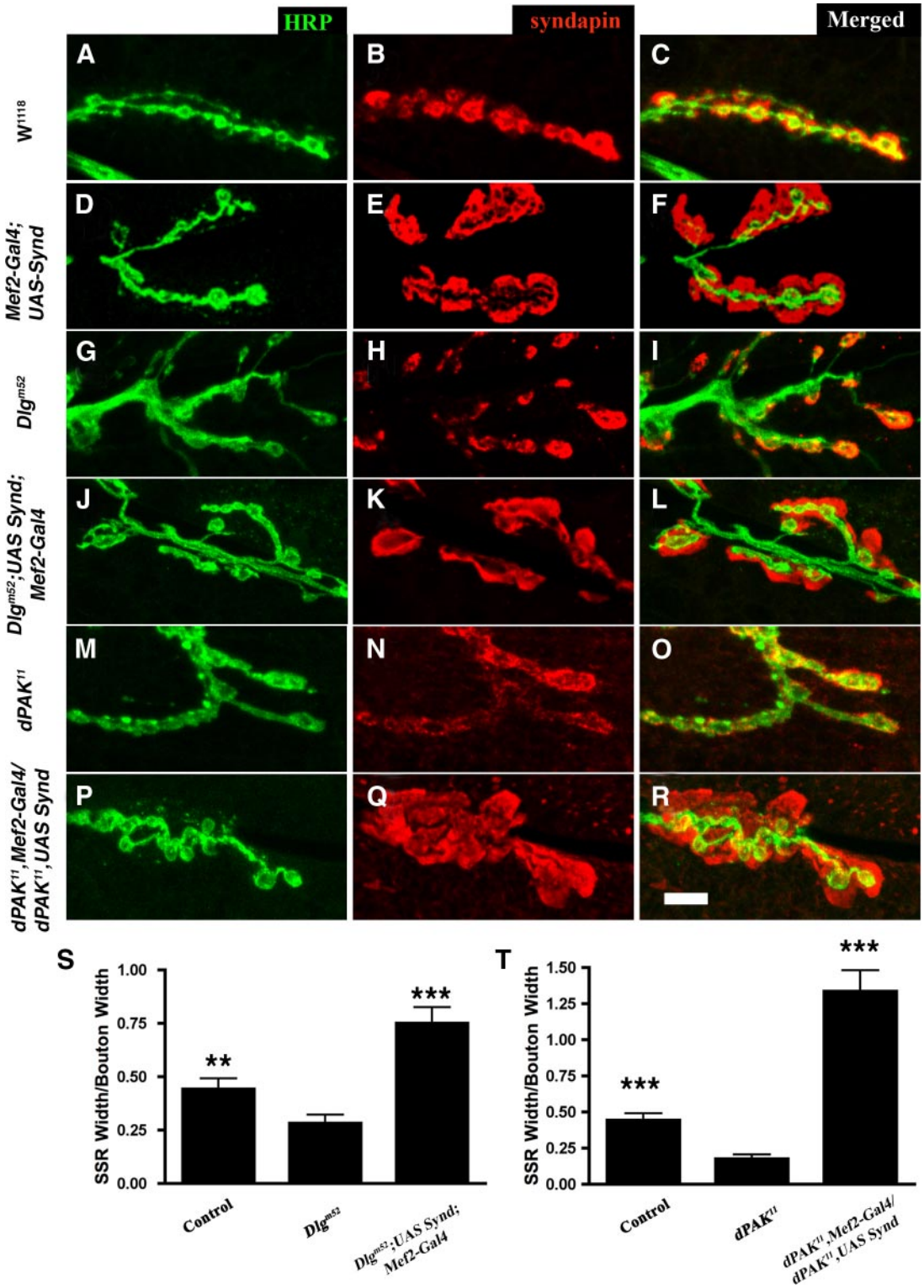

Figure 5. Syndapin-mediated SSR expansion does not require Dlg or dPAK. (A–O) Third instar larval NMJ of wild-type (A–C), *Mef2-Gal4; UAS-syndapin* (D–F), Dlg^{m52} (G–I), Dlg^{m52}*; UAS-syndapin; Mef2-Gal4* (J–L), $dPAK^{11}$ (M–O), and $dPAK^{11}$, *Mef2-Gal4/*$dPAK^{11}$, *UAS-syndapin* (P–R) genotypes, colabeled for HRP (green) and syndapin (red). The underdeveloped SSR defects (as assayed by syndapin immunoreactivity and membrane labeling around boutons) of *Dlg* (G–I) and *dPAK* (M–O) were rescued by syndapin expression in the muscles. (S) Quantification of normalized SSR width in control (0.44 ± 0.05; n = 18 boutons), Dlg^{m52} (0.28 ± 0.04; n = 21 boutons), and Dlg^{m52}*; UAS-syndapin; Mef2-Gal4* (0.75 ± 0.074; n = 13 boutons). (T) Quantification of normalized SSR width in control (0.44 ± 0.05; n = 18 boutons), $dPAK^{11}$ (0.18 ± 0.03; n = 12 boutons), and $dPAK^{11}$, *UAS-syndapin/*$dPAK^{11}$, *Mef2-Gal4* (1.34 ± 0.1; n = 19 boutons). Normalization was done by dividing the SSR width by respective bouton width. Bar, 10 μm (in R) for A–R. Error bars represent SEM. **$p < 0.01$, ***$p < 0.0001$.

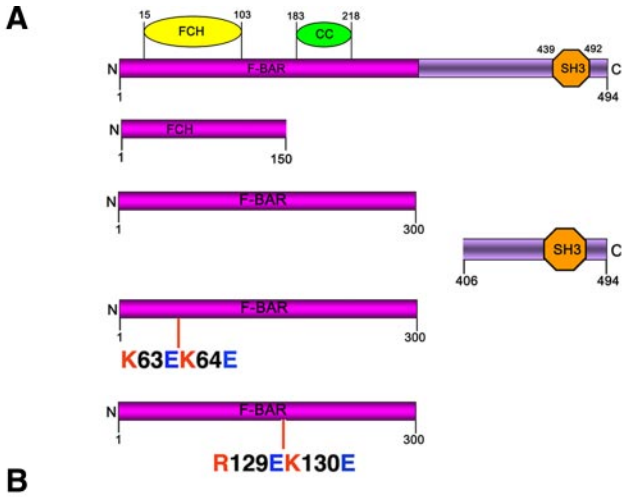

C

	Tubulation
syndapin full (1-494)	+
syndapin (1-150)	-
syndapin (1-300)	+++
syndapin (1-300 K63EK64E)	-
syndapin (1-300 R129EK130E)	-
syndapin (406-494)	-

B

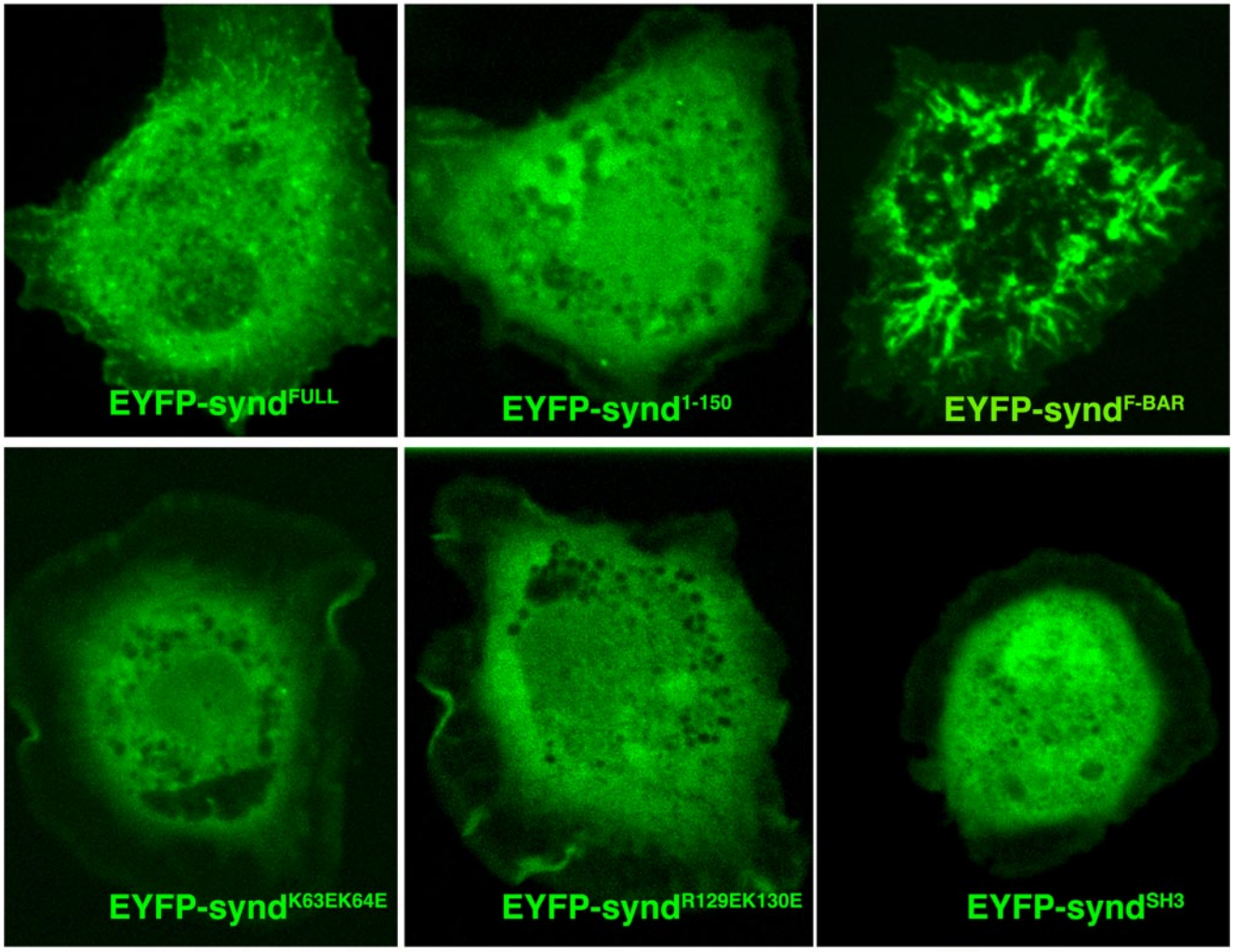

Figure 6. Tubulation effect of *Drosophila* syndapin and its mutants in S2 cultured cells. (A) Domains and mutants of syndapin expressed as fusions to EYFP. Syndapin has an N-terminal F-BAR domain consisting of FCH and coiled-coil (CC) domain and an SH3 toward its C terminus. (B) S2 cells were transfected with N-terminal EYFP-tagged constructs of syndapin. The localization of protein was visualized by EYFP fluorescence. Note the massive induction of tubulation by the F-BAR domain of syndapin in S2 cells. (C) Relative tubulation ability of the various syndapin constructs in S2 cells expressed as +++ (very strong), + (weak/detectable), and − (no tubulation).

Does SSR biogenesis induced by syndapin reflect its true physiological function rather than an interesting but physiologically irrelevant activity of the protein? The SSR remains normal in *synd* loss-of-function mutants. Although this

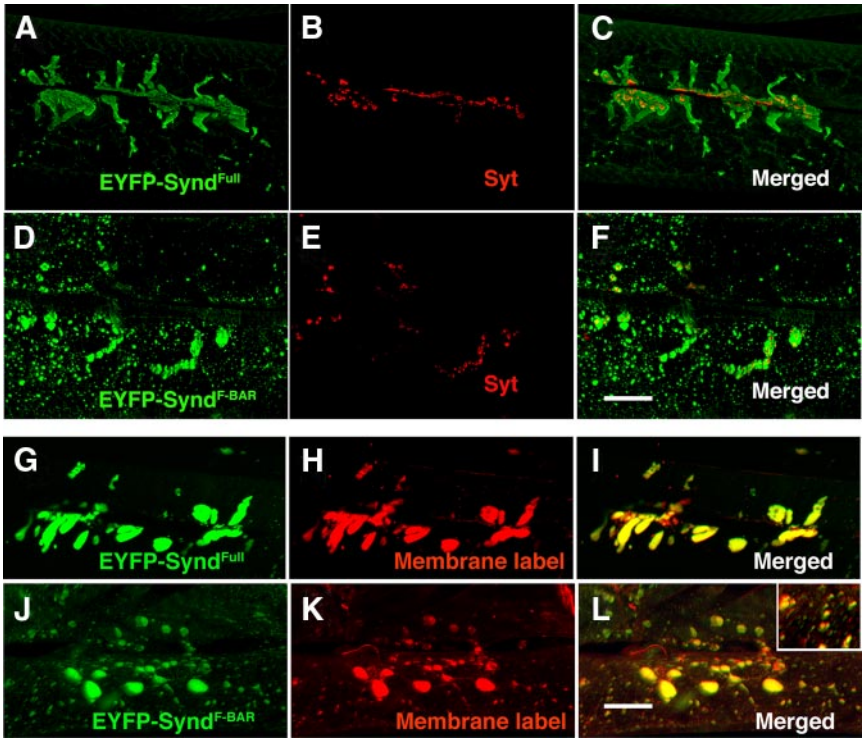

Figure 7. Syndapin-mediated SSR expansion requires Synd targeting to NMJ by its SH3 domain. (A–C) Projected confocal image of EYFP-tagged full-length syndapin expressed in muscle, colabeled for EYFP (A) and presynaptic marker synaptotagmin (B). Note that extrasynaptic syndapin remain in close vicinity to presynaptic terminals and is not randomly distributed through out the muscle surface. (D–F) Projected confocal image of EYFP-tagged F-BAR domain of syndapin expressed in muscle, colabeled for EYFP (D) and presynaptic marker synaptotagmin (F). Note that syndapin immunoreactivity is randomly distributed in patches through out the muscle surface and very little Synd$^{F\text{-}BAR}$ is targeted to NMJs. (G–I) Projected confocal image of EYFP-tagged full-length syndapin expressed in muscles, labeled for EYFP (G) and membrane (H) by using FM1-43. (I) Merged image of G and H. (J–L) Projected confocal image of EYFP-tagged F-BAR domain (residues 1-300) of syndapin expressed in muscles, labeled for EYFP (J) and membrane (K) by using FM1-43. Note the presence of many small EYFP-containing membrane domains scattered over the entire muscle. (L) Merged image of J and K. Note that EYFP-tagged F-BAR of syndapin does not efficiently get targeted to NMJ and induces random patches of membranes throughout muscle surface (see inset in L). Bar, 30 μm (in F) for A–F and 20 μm (in L) for G–L.

could suggest that Synd has no physiological function in SSR biogenesis, an alternative possibility is that other postsynaptic F-BAR proteins compensate for the absence of syndapin. Indeed, potential functional redundancies among

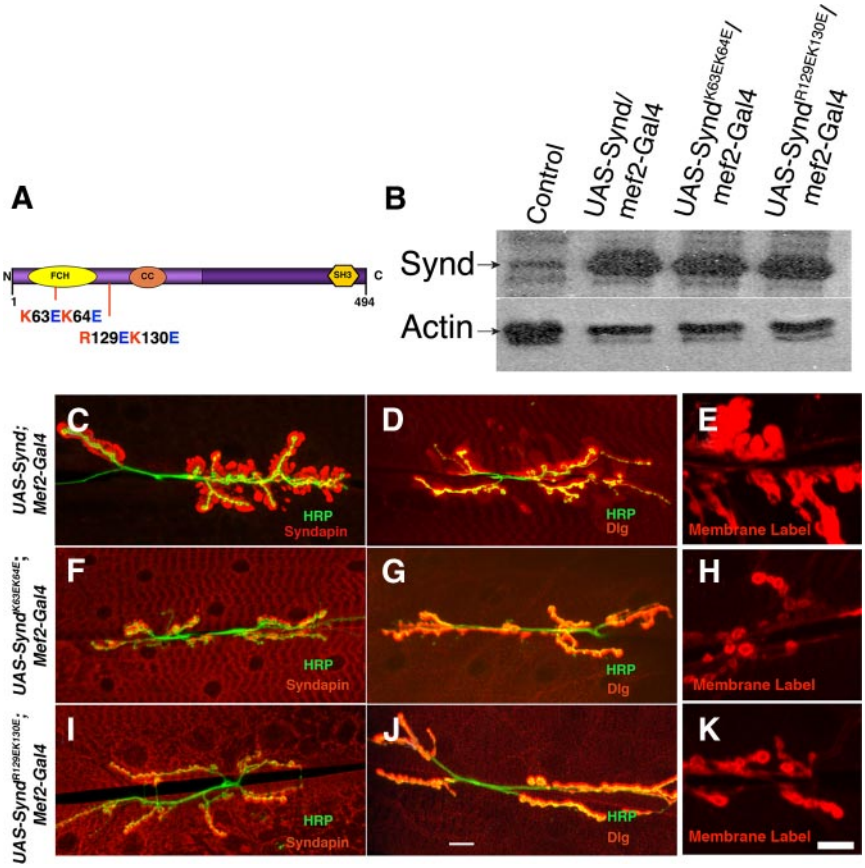

Figure 8. Syndapin-mediated SSR expansion critically requires syndapin's F-BAR domain interactions with muscle membrane. (A) Positions of basic amino acid residues predicted to be essential for F-BAR membrane interactions. In the *K63EK64E* mutant syndapin, the lysine residues, K63 and K64 were mutated to glutamic acid (E). Similarly, in the *R129EK130E* mutant, arginine and lysine residues, R129 and K130 were mutated to glutamic acid. (B) Western blot of *Drosophila* third instar larval lysates of control or of various syndapin transgenes overexpressing in muscles, probed with anti-Synd antibody. Mutant syndapin transgenes express to comparable level to wild-type transgene. Actin was used as loading control. (C–E) Confocal images of muscle overexpressing wild-type syndapin colabeled with anti-Synd and anti-HRP (C) or anti-HRP and anti-Dlg (D), showing expansions of synaptic and extrasynaptic SSR, or membrane marker FM1-43 (E). (F–H) Similar images of muscle overexpressing mutant syndapin (Synd^{K63EK64E}) transgene, colabeled with anti-Synd and anti-HRP (F) or anti-HRP and anti-Dlg (G) or membrane marker FM1-43 (H). Note that Dlg and FM1-43–positive synaptic and extrasynaptic SSRs are not induced. (I–K) Confocal images of muscle overexpressing mutant syndapin (Synd^{R129EK130E}) transgene, colabeled with anti-Synd and anti-HRP (I) or anti-HRP and anti-Dlg (J) or membrane marker FM1-43 (K). Note that like Synd^{K63EK64E}, Dlg- and FM1-43–positive synaptic and extrasynaptic SSRs are not induced. Bar, 15 μm (in J) for C, D, F, G, I, and J. Bar, 15 μm (in K) for E, H, and K.

F-BAR proteins are suggested by reports that different F-BAR proteins can coexist on a single tubule (Frost *et al*., 2008).

Although alternative models are tenable, we suggest that Synd has a role in SSR biogenesis in vivo based on four arguments. First, Synd is localized to the postsynaptic SSR and would therefore most simply be expected to have an SSR-related function. The observed expansion of the SSR is consistent with this premise. Second, full-length Synd overexpression does not cause random patches of SSR to be induced all over the muscle surface but rather causes local expansions as well as flares that often seem to emanate from the existing SSR. Thus, the observed consequence of Synd overexpression seems to originate from sites to which Synd is normally targeted in vivo. Third, that Synd can promote formation of a unique, highly complex membrane system in vivo indicates that it participates in intricate processes that likely require the coordinated function of many different proteins. Finally, consistent with the previous argument, muscle expression of other *Drosophila* F-BAR domain proteins such as Nervous wreck (Coyle *et al*., 2004) (Supplemental Figure S4) or Cip4 (data not shown) does not induce SSR expansion.

Syndapin Decouples Membrane Tubulation and Fission for SSR Expansion

In cultured cells, overexpression of F-BAR proteins induces transient, dynamin-containing plasma membrane tubules that are rapidly fragmented by dynamin-mediated membrane scission (Itoh *et al*., 2005; Tsujita *et al*., 2006). Here, tubulation can be decoupled from membrane fission only if either the SH3 domain is removed or if SH3 interacting molecules (e.g., dynamin) are inhibited. A physiological decoupling of membrane tubulation and fission activities has been shown previously for the N-BAR domain proteins, mouse Amphiphysin 2 and *Drosophila* Amphiphysin, during T-tubule formation (Razzaq *et al*., 2001; Lee *et al*., 2002). Our observations suggest that similar physiological decoupling of the two activities—membrane deformation and membrane fission also occurs for the syndapin, an F-BAR domain protein.

In support of this, we show that unlike synd, the membrane fission protein dynamin is not enriched in the SSR (Supplemental Figure S2); this is different from strong colocalization observed between dynamin and syndapin in transient tubules in cultured cells. Furthermore, the presence of the dynamin-interacting SH3 domain does not inhibit syndapin's ability to promote SSR formation. Thus, in contrast to prior observations in cultured cells, our data show that syndapin in vivo can 1) be present without accompanying dynamin and 2) can form stable membrane infoldings without need to experimentally inhibit SH3 domain interactions.

Syndapin Uses Conserved Basic Amino Acid Residues to Promote SSR Expansion

The mechanism by which syndapin promotes SSR formation is likely to require direct membrane interactions mediated by previously identified residues on the concave face of its F-BAR domain. Mutations in key residues on the concave face of the F-BAR domain, required for phospholipid binding, block the ability of syndapin to induce SSR. Thus, mechanisms that underlie F-BAR protein's ability to tubulate membrane in vitro seem to be required for syndapin's ability to expand the SSR. However, Synd-induced SSR formation requires additional events, including correct targeting to the postsynapse, a function that requires the C-terminal SH3 domain.

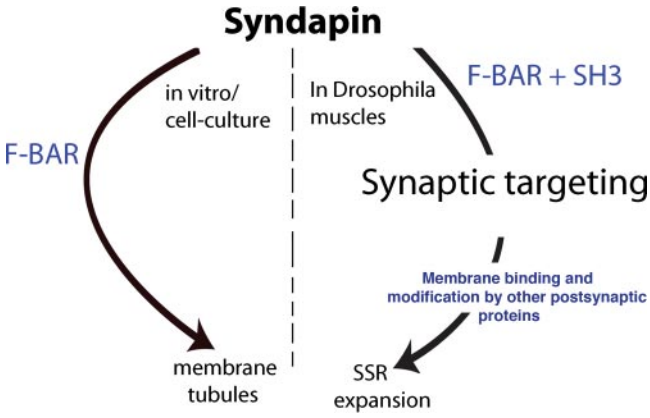

Figure 9. A simple model showing how syndapin expands SSR at NMJs. In in vivo and cell-cultures, the F-BAR domain of syndapin is sufficient to induce membrane tubules. However, at the *Drosophila* neuromuscular junctions, the F-BAR as well as SH3 domains are required for proper targeting of syndapin to the NMJs. Once properly targeted, syndapin is retained there and generates new tubulolamellar structures by a mechanism that involves F-BAR domain binding to the muscle membranes through its conserved positively charged residues. Other SSR-enriched proteins, which may potentially be targeted through syndapin's SH3 domain interaction, may subsequently modify the tubulolamellar structures generated by syndapin.

Although Synd lacking its SH3 domain is extremely efficient at membrane tubulation/remodeling in S2 cells, this truncated protein is not postsynaptically targeted in muscle cells and is ineffective for SSR expansion. Thus, the SH3 domain of Synd must interact with targeting molecules that control syndapin's postsynaptic localization. By extension, the targeting of other F-BAR domain proteins, which may be mediated by analogous SH3 domain interactions, could be important for their respective in vivo functions. A simple model explaining and summarizing our observation on syndapin is presented as Figure 9.

Could our observations on syndapin be relevant to the function of other F-BAR domain proteins? The SSR has some similarity to plasma membrane specializations such as the demarcation membrane system of megakaryocytes, which give rise to platelet plasma membrane (Tolhurst *et al*., 2005). It is conceivable that other F-BAR domain proteins will be found to be involved in the biogenesis of these or other complex membrane system. Further studies are required to understand the different processes involved in SSR biogenesis and also to test the relevance of these findings to other members of the F-BAR protein family.

ACKNOWLEDGMENTS

We thank Drs. Eyal Schejter, Vivian Budnik, and Aaron DiAntonio; the Szeged and Bloomington stock centers; and the Developmental Studies Hybridoma Bank for reagents. We thank Drs. Barry Ganetzky, Ian Coyle, Ullrich Thomas and Iain Robinson for sharing unpublished observations. We also thank Dr. Francis Chee and Carl Boswell for help with confocal microscopy, Shobha Ramagiri for electron microscopy, and Drs. Subhabrata Sanyal and Konrad Zinsmaier for many useful comments on the manuscript. This work, supported by a Project grant from the Wellcome Trust, was initiated with support from the Science Foundation of Ireland, the National Institute on Drug Abuse/National Institutes of Health, and endowment funds from the Tata Institute of Fundamental Research.

REFERENCES

Albin, S. D., and Davis, G. W. (2004). Coordinating structural and functional synapse development: postsynaptic p21-activated kinase independently spec-

ifies glutamate receptor abundance and postsynaptic morphology. J. Neurosci. *24*, 6871–6879.

Atwood, H. L., Govind, C. K., and Wu, C. F. (1993). Differential ultrastructure of synaptic terminals on ventral longitudinal abdominal muscles in *Drosophila* larvae. J. Neurobiol. *24*, 1008–1024.

Bogdan, S., and Klambt, C. (2003). Kette regulates actin dynamics and genetically interacts with Wave and Wasp. Development *130*, 4427–4437.

Budnik, V., Koh, Y. H., Guan, B., Hartmann, B., Hough, C., Woods, D., and Gorczyca, M. (1996). Regulation of synapse structure and function by the *Drosophila* tumor suppressor gene dlg. Neuron *17*, 627–640.

Coyle, I. P., Koh, Y. H., Lee, W. C., Slind, J., Fergestad, T., Littleton, J. T., and Ganetzky, B. (2004). Nervous wreck, an SH3 adaptor protein that interacts with Wsp, regulates synaptic growth in *Drosophila*. Neuron *41*, 521–534.

Dawson, J. C., Legg, J. A., and Machesky, L. M. (2006). Bar domain proteins: a role in tubulation, scission and actin assembly in clathrin-mediated endocytosis. Trends Cell Biol. *16*, 493–498.

Farsad, K., and De Camilli, P. (2003). Mechanisms of membrane deformation. Curr. Opin. Cell Biol. *15*, 372–381.

Frost, A., Perera, R., Roux, A., Spasov, K., Destaing, O., Egelman, E. H., De Camilli, P., and Unger, V. M. (2008). Structural basis of membrane invagination by F-BAR domains. Cell *132*, 807–817.

Gorczyca, D., Ashley, J., Speese, S., Gherbesi, N., Thomas, U., Gundelfinger, E., Gramates, L. S., and Budnik, V. (2007). Postsynaptic membrane addition depends on the Discs-Large-interacting t-SNARE Gtaxin. J. Neurosci. *27*, 1033–1044.

Guan, B., Hartmann, B., Kho, Y. H., Gorczyca, M., and Budnik, V. (1996). The Drosophila tumor suppressor gene, dlg, is involved in structural plasticity at a glutamatergic synapse. Curr. Biol. *6*, 695–706.

Habermann, B. (2004a). The BAR-domain family of proteins: a case of bending and binding? EMBO Rep. *5*, 250–255.

Habermann, B. (2004b). The BAR-domain family of proteins: a case of bending and binding? EMBO Rep. *5*, 250–255.

Itoh, T., Erdmann, K. S., Roux, A., Habermann, B., Werner, H., and De Camilli, P. (2005). Dynamin and the actin cytoskeleton cooperatively regulate plasma membrane invagination by BAR and F-BAR proteins. Dev. Cell *9*, 791–804.

Kessels, M. M., and Qualmann, B. (2002). Syndapins integrate N-WASP in receptor-mediated endocytosis. EMBO J. *21*, 6083–6094.

Kessels, M. M., and Qualmann, B. (2004). The syndapin protein family: linking membrane trafficking with the cytoskeleton. J. Cell Sci. *117*, 3077–3086.

Kessels, M. M., and Qualmann, B. (2006). Syndapin oligomers interconnect the machineries for endocytic vesicle formation and actin polymerization. J. Biol. Chem. *281*, 13285–13299.

Kumar, V., Alla, S. R., Krishnan, K. S., and Ramaswami, M. (2008). Syndapin is dispensable for synaptic vesicle endocytosis at the *Drosophila* larval neuromuscular junction. Mol. Cell Neurosci.

Lahey, T., Gorczyca, M., Jia, X. X., and Budnik, V. (1994). The *Drosophila* tumor suppressor gene dlg is required for normal synaptic bouton structure. Neuron *13*, 823–835.

Lee, E., Marcucci, M., Daniell, L., Pypaert, M., Weisz, O. A., Ochoa, G. C., Farsad, K., Wenk, M. R., and De Camilli, P. (2002). Amphiphysin 2 (Bin1) and T-tubule biogenesis in muscle. Science *297*, 1193–1196.

McMahon, H. T., and Gallop, J. L. (2005). Membrane curvature and mechanisms of dynamic cell membrane remodelling. Nature *438*, 590–596.

Mendoza, C., Olguin, P., Lafferte, G., Thomas, U., Ebitsch, S., Gundelfinger, E. D., Kukuljan, M., and Sierralta, J. (2003). Novel isoforms of Dlg are fundamental for neuronal development in *Drosophila*. J. Neurosci. *23*, 2093–2101.

Parnas, D., Haghighi, A. P., Fetter, R. D., Kim, S. W., and Goodman, C. S. (2001). Regulation of postsynaptic structure and protein localization by the Rho-type guanine nucleotide exchange factor dPix. Neuron *32*, 415–424.

Perez-Otano, I., Lujan, R., Tavalin, S. J., Plomann, M., Modregger, J., Liu, X. B., Jones, E. G., Heinemann, S. F., Lo, D. C., and Ehlers, M. D. (2006). Endocytosis and synaptic removal of NR3A-containing NMDA receptors by PACSIN1/syndapin1. Nat. Neurosci. *9*, 611–621.

Peter, B. J., Kent, H. M., Mills, I. G., Vallis, Y., Butler, P. J., Evans, P. R., and McMahon, H. T. (2004). BAR domains as sensors of membrane curvature: the amphiphysin BAR structure. Science *303*, 495–499.

Pielage, J., Fetter, R. D., and Davis, G. W. (2006). A postsynaptic spectrin scaffold defines active zone size, spacing, and efficacy at the *Drosophila* neuromuscular junction. J. Cell Biol. *175*, 491–503.

Razzaq, A., Robinson, I. M., McMahon, H. T., Skepper, J. N., Su, Y., Zelhof, A. C., Jackson, A. P., Gay, N. J., and O'Kane, C. J. (2001). Amphiphysin is necessary for organization of the excitation-contraction coupling machinery of muscles, but not for synaptic vesicle endocytosis in *Drosophila*. Genes Dev. *15*, 2967–2979.

Shibata, Y., Voeltz, G. K., and Rapoport, T. A. (2006). Rough sheets and smooth tubules. Cell *126*, 435–439.

Shimada, A., *et al*. (2007). Curved EFC/F-BAR-domain dimers are joined end to end into a filament for membrane invagination in endocytosis. Cell *129*, 761–772.

Simpson, F., Hussain, N. K., Qualmann, B., Kelly, R. B., Kay, B. K., McPherson, P. S., and Schmid, S. L. (1999). SH3-domain-containing proteins function at distinct steps in clathrin-coated vesicle formation. Nat. Cell Biol. *1*, 119–124.

Stowell, M. H., Marks, B., Wigge, P., and McMahon, H. T. (1999). Nucleotide-dependent conformational changes in dynamin: evidence for a mechanochemical molecular spring. Nat. Cell Biol. *1*, 27–32.

Takano, K., Toyooka, K., and Suetsugu, S. (2008). EFC/F-BAR proteins and the N-WASP-WIP complex induce membrane curvature-dependent actin polymerization. EMBO J. *27*, 2817–2828.

Tolhurst, G., Vial, C., Leon, C., Gachet, C., Evans, R. J., and Mahaut-Smith, M. P. (2005). Interplay between P2Y(1), P2Y(12), and P2X(1) receptors in the activation of megakaryocyte cation influx currents by ADP: evidence that the primary megakaryocyte represents a fully functional model of platelet P2 receptor signaling. Blood *106*, 1644–1651.

Tsujita, K., Suetsugu, S., Sasaki, N., Furutani, M., Oikawa, T., and Takenawa, T. (2006). Coordination between the actin cytoskeleton and membrane deformation by a novel membrane tubulation domain of PCH proteins is involved in endocytosis. J. Cell Biol. *172*, 269–279.

Wigge, P., and McMahon, H. T. (1998). The amphiphysin family of proteins and their role in endocytosis at the synapse. Trends Neurosci. *21*, 339–344.

Zimmerberg, J., and Kozlov, M. M. (2006). How proteins produce cellular membrane curvature. Nat. Rev. Mol. Cell. Biol. *7*, 9–19.

Zinsmaier, K. E., Eberle, K. K., Buchner, E., Walter, N., and Benzer, S. (1994). Paralysis and early death in cysteine string protein mutants of *Drosophila*. Science *263*, 977–980.

Zinsmaier, K. E., Hofbauer, A., Heimbeck, G., Pflugfelder, G. O., Buchner, S., and Buchner, E. (1990). A cysteine-string protein is expressed in retina and brain of *Drosophila*. J. Neurogenet. *7*, 15–29.